Bi-Functional Antenna Coating for Cloaking and Directivity Enhancement Made of Isotropic Materials

Mohammad H. Fakheri[1, 2], Ali Abdolali[1, 2, *], Zohreh Moradinia[1, 2], Homayoon Oraizi[1], and Ali Keivaan[1]

Abstract—In this paper, using quasi-conformal mapping, a bi-functional coating layer is designed with the intention of both cloaking and directivity enhancement of an omnidirectional antenna. For TM external waves coming from a certain direction, the proposed coating layer conceals the inner objects. In addition to the cloaking performance, the designed coating layer plays the role of a metamaterial-based lens that dramatically enhances the directivity level of inner omnidirectional loop-family antennas. To reach this goal, a proper coordinate transformation is elaborately utilized to transform the cylindrical wavefronts radiated from the antenna into semi-pure plane waves. With appropriate simplifications, the proposed coating layer turns into an isotropic meta-device, which is more suitable to be fabricated. To prove the feasibility of the implementation, an SRR-meander line meta-atom is designed to locally realize the required permittivity and permeability distribution of the bi-functional layer. Full-wave simulations are performed via COMSOL finite element solver to validate the cloaking effect and directivity enhancement of the proposed coating layer, at the same time.

1. INTRODUCTION

The control of electromagnetic waves in the desired path is conceivable by using the powerful concept of transformation optics (TO) [1]. Based on the form-invariant Maxwell's equations and appropriate coordinate transformation, a new transformed space can be created with desired electromagnetic properties [2]. The relations between coordinate transformations and materials parameters dates back to 1961 [3]. However, until the introduction of metamaterials, such relation was generally considered as a mathematical technique. As an example, to facilitate the solution of particular problems, e.g., helicoidal geometries, non-orthogonal coordinate transformation may be suitable [4]. Afterward, the TO concept has resulted in the development of numerous devices such as EM wave concentrators which play a significant role in the harnessing of energy in solar cells, where high field intensities are needed [5]. Moreover, TO has been combined with microwave devices such as waveguide bend, which connects two waveguides even with different size at different angles without any EM field perturbations [6]. Besides, the theory of TO opens up new horizons for the antenna designs like antenna lens [7], antenna beam steering [8] and antenna pattern synthesis [9]. In [9] the authors propound a general approach for enabling the customizable multiple beam radiation of planar antennas. Among all these applications, the invisibility cloak is one of the most interesting TO-based devices, which conceals interior objects [10, 11]. These perfect cloaks compress part of the space to a point or line in spherical [10] or cylindrical cloaks [12], respectively. Since the scattering from a highly conducting point or line is negligible, these cloaks hide the object perfectly [13]. However, the required materials for perfect cloaks have singularities and need a wide range of material properties, which have limited their applications

in practical scenarios. To overcome this issue, another kind of cloaking named "carpet cloak" was introduced by Pendry [13]. It compresses part of the space to a ground plane and thus makes the underneath objects behave like a flat conducting plane and consequently undetectable. As the obtained material parameters have a narrower range of permittivity and permeability, it could become more experimentally realizable in two- and three-dimensions [14–16]. "Unidirectional cloaks" with promising features of cloaking the objects in free space, while having realizable material parameters are presented in [17–21]. In this type of invisibility cloak, a part of space is transformed into an infinitesimal PEC surface. It conceals the inside objects from the TM waves (with H_z polarization) along the surface direction since TM waves have no scattering when incident onto a PEC surface. Besides, the development of metasurfaces as the two-dimensional version of metamaterials have attracted great attention due to their simple fabrication and powerful capabilities to control the EM waves [22]. Due to their ability to control the characteristic discontinuities at the surface, including phase, amplitude, and polarization of EM fields, one can fully mold the EM waves in reflection [23] or transmission mode [24, 25]. Moreover, metasurfaces have paved the way towards achieving invisibility cloaks with less occupying space in comparison with their counterparts, i.e., metamaterials [26–28]. However, they are effective for scatterer dimensions in the quasi-static regime [29]. Recently metasurface cloaks have been utilized to reduce electromagnetic interference among different antennas and their blockage effects [30, 31].

Moreover, TO-based devices typically lead to anisotropic and inhomogeneous electromagnetic characteristics. To overcome this challenge many efforts have been made using quasi-conformal (QC) mappings [13, 15, 32, 33]. This technique results in isotropic cloak for specific polarization, which is more practical and realizable. On the other hand, the shape of an object being cloaked is not always simple and requires implementing challenging techniques [34]. In order to determine the constitutive parameters of the cloak, a partial differential equation (PDE), such as Laplace equation, is solved under proper boundary conditions, regardless of shape of layer [35].

The modification of radiation properties of electromagnetic sources is another application of TO, which is appropriate for wireless communication systems such as base station antennas. A variety of techniques are employed for this purpose [36, 37]. In [36] based on an embedded optical transformation, a metamaterial lens is proposed which converts cylindrical waves into plane waves. A conversion of the cylindrical waves emitted by a line source into a directive multi-beam emission is performed by homogeneous metamaterials based on linear transformation [37, 38]. To enable broadband and low-loss devices, quasi-conformal TO-based lenses are introduced, which lead to isotropic non-magnetic materials [39, 40].

The proposed structure in [21] has the merit of simultaneously achieving both the cloaking and directivity enhancement for a cylindrical antenna. However, the realization of complex anisotropic and inhomogeneous media is difficult. Using quasi-conformal mapping for such layers is appropriate in that it simplifies the medium to an isotropic material. In this paper a coating layer is proposed which combines two different functions in a single device based on the quasi-conformal mapping. This bi-functional device cloaks an omnidirectional antenna from TM waves along a specified direction. This functionality is applicable, particularly in multiple antenna environments, where it is desirable to reduce the mutual coupling effects among adjacent antennas. In addition, this layer enhances the directivity of an enclosed omnidirectional parallel-polarized antenna where its magnetic field is along the antenna axis. The proposed coating layer has an arbitrary shape consists of an isotropic material, as advantages of quasi-conformal mapping, which is performed by solving the Laplace equation with proper boundary conditions. Near-field and far-field simulations are performed by COMSOL finite element solver to validate the bi-functionality features of the proposed layer. Finally, to show the possibility of realization, a composite of SRR-meander line array is employed which drastically facilitates the physical realization of the proposed coating layer.

2. DESIGN METHOD

The basic idea of proposed concept is to cloak an omnidirectional parallel-polarized antenna from TM-polarized waves while making its omnidirectional pattern to a highly directive emission. Fig. 1 shows the coordinate transformation from the virtual space to the physical one. As can be seen, a hole is made in the space by the QC mapping in a way that the vertical lines become orthogonal to the hole
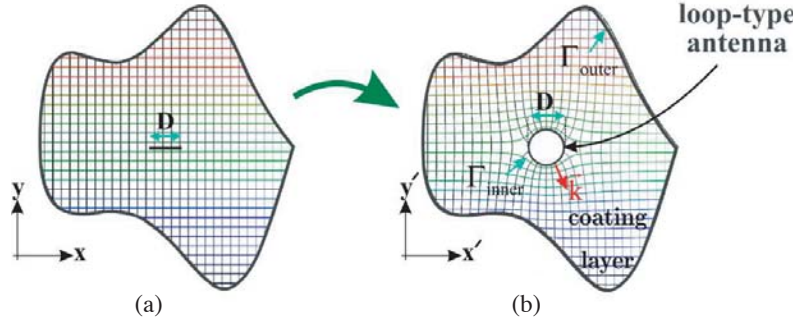
Figure 1. Schematic diagram of coordinate transformation using quasi-conformal mapping. (a) Virtual space; (b) Physical space.

and the horizontal lines encircle it. By mapping a line segment to a circle in the interior boundary, and keeping the exterior boundary (with arbitrary shape) unchanged, the virtual space will be compressed into the physical one. Since the exterior boundary configurations in the physical and virtual spaces are identical (see Fig. 1), the rectangular grids near the outer boundary regions are the same in both spaces. When an omnidirectional antenna is placed at the marked circle (which is represented by the whole inner boundary), its wavefronts will be matched to the horizontal lines.

Why cylindrical waves convert into plane waves at the end of the cloak region is originated from the fact that the circular curves along with the horizontal axis gradually convert into the straight lines in the vicinity of exterior boundaries. Indeed, due to the grid orthogonality in the physical space, the propagation vector along vertical lines will be perpendicular to the equiphase plane, which matches with the horizontal lines. Fig. 1(b) demonstrates that when a cylindrical wave propagates along with longitudinal coordinates, its latitudinal component becomes zero. Therefore, the omnidirectional antenna changes to a directive one. Besides, when the E_y-polarized incident wave illuminates the structure along the horizontal direction, it rounds the cloaked space with unchanged phase front and makes the enclosed antenna invisible from external EM sources, simultaneously. The PEC circle acts as if there is a flat PEC surface, which is rooted in the mapping of the PEC linear segment into the circular shape. Hence, there will be no scattering or diffraction due to the fact that the electric field with E_y component and the conductor surface are orthogonal.

The constitutive materials of the physical space can be obtained using Maxwell's equations [1, 3, 4]:

$$\bar{\bar{\varepsilon}}' = \frac{\bar{\bar{A}}\varepsilon\bar{\bar{A}}^T}{\det \bar{\bar{A}}}, \quad \bar{\bar{\mu}}' = \frac{\bar{\bar{A}}\mu\bar{\bar{A}}^T}{\det \bar{\bar{A}}} \tag{1}$$

where A is the Jacobian matrix in the transformed space with the components $A_{ij} = \partial x'_i / \partial x_j$. The Jacobean matrix determines the geometrical transformations between the virtual and physical spaces. As stated in [13] and [27], when all the local coordinate systems in the transformed medium are quasi-orthogonal, the designed structure can be realized with isotropic materials. In order to generate an orthogonal two-dimensional grid, the off-diagonal components of the metric tensor g, are identical to zero, which means that [41]:

$$g_{21} = g_{12} = \frac{\partial x}{\partial x'}\frac{\partial x}{\partial y'} + \frac{\partial y}{\partial x'}\frac{\partial y}{y'} = 0 \tag{2}$$

Solving Eq. (2) with Neumann-Dirichlet boundary conditions guarantees the orthogonality condition. This can be achieved with the PDE solver of commercial finite element based COMSOL MULTIPHYSICS software. A proper boundary specification for this problem leads to a bi-functional layer. In order to have no reflection from the cloaking layer, the exterior boundaries should set to be $x'|_{\Gamma_{outer}} = x$, $y'|_{\Gamma_{outer}} = y$, without any change, whilst the inner boundary (with circle shape) is mapped into a linear segment on $y = 0$. The length of the line segment and the diameter of the circle are the same. So its boundary condition is $y'|_{\Gamma_{inner}} = 0$ and $\hat{n} \cdot (\nabla x')|_{\Gamma_{inner}} = 0$. The latter condition assures that the grids are orthogonal in the inner boundary as shown in Fig. 1.

With the assumption of H_z-polarized wave, only ε_{xx}, ε_{yy}, ε_{xy}, ε_{yx}, and μ_{zz} components contribute in both functionalities. Therefore, the permittivity and permeability of the coating layer under the aforementioned condition (Eq. (2)) become [32]:

$$\varepsilon' = 1, \quad \mu' = \mu_{zz} = {}^1\!/\!\det(A) \tag{3}$$

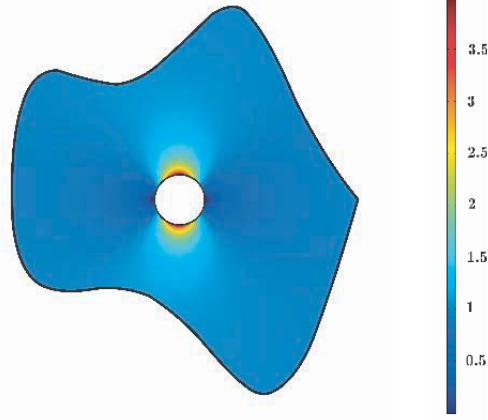where the distribution of μ' is shown in Fig. 2.

Figure 2. Relative permeability map of the bi-functional cloak.

3. NUMERICAL RESULTS AND DISCUSSION

Numerical simulations at the microwave spectrum have been employed using finite element based COMSOL MULTIPHYSICS software to verify the performance of the bi-functional device. Since the outer radiation boundary is a rectangle with the size of $0.7 \, \text{m} \times 1 \, \text{m}$, the provided simulations exhibit both near field and far-field behavior of the structure. The bi-functional coating layer has an arbitrary shape with the hole radius of $r = 0.03 \, \text{m}$. At the first step, to investigate the directivity enhancement, an omnidirectional loop-type antenna with operating frequency of $3.5 \, \text{GHz}$ is placed at the center of coating layer in contact with the inner boundary.

A loop-type antenna with a cylindrical wavefront is illustrated in Fig. 3(a). This antenna radiates an omnidirectional pattern, which is shown in Fig. 4(a). As mentioned earlier, by covering the loop-family antennas with the proposed material, the phase fronts will be gradually transformed from cylindrical to
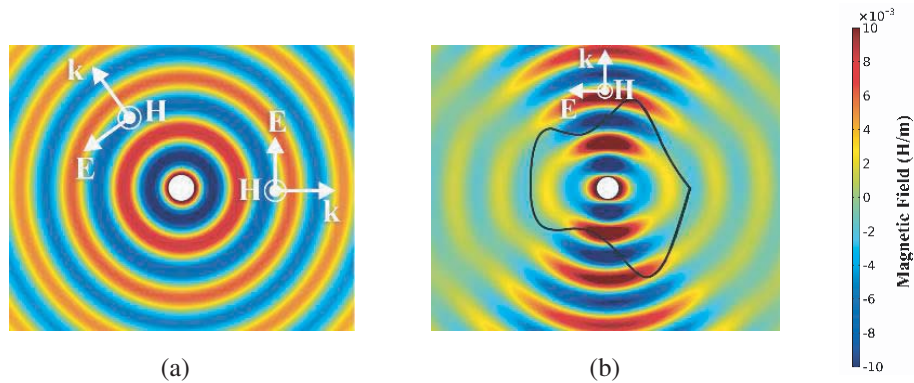

Figure 3. The magnetic field distribution at $3.5 \, \text{GHz}$ for (a) loop antenna in free space and (b) loop antenna covered with the proposed material.
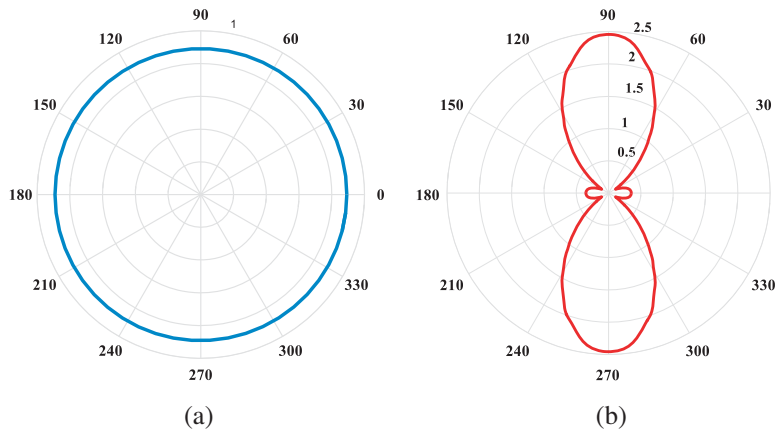
Figure 4. Far-field pattern at $3.5\,\text{GHz}$ of (a) loop antenna in free space and (b) loop antenna covered with the proposed material.
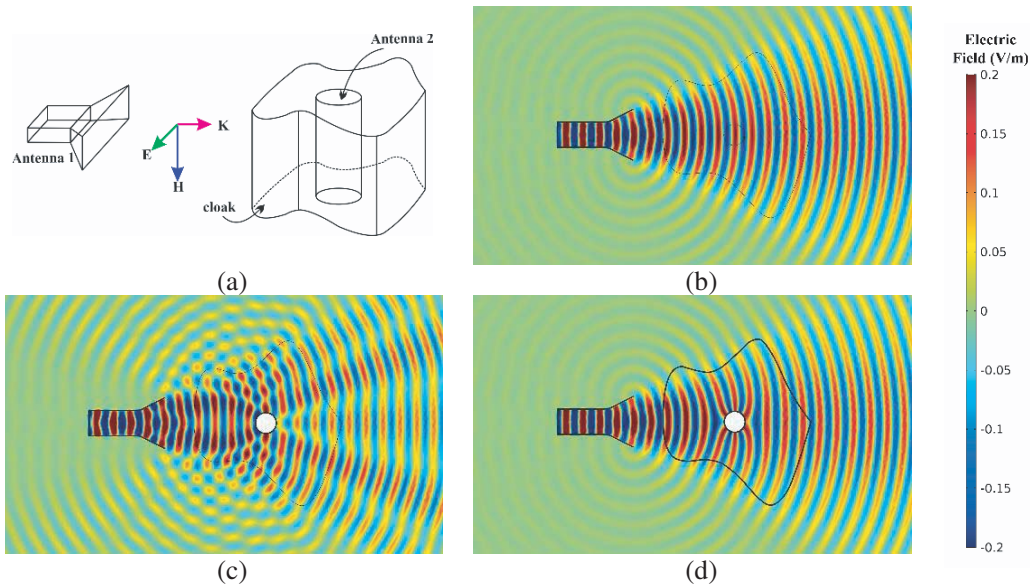

Figure 5. The electric field distribution radiated by the horn antenna at $10.5\,\text{GHz}$ (antenna 1): (a) the schematic of multiple antenna environment and the proposed method for coupling reduction. (b) Radiating fields from antenna 1 in free space. (c) Radiating fields from antenna 1 in the presence of loop-type antenna (antenna 2). (d) Antenna 2 is covered by the proposed layer.

plane waves at the end. This is due to the slight change in the grid lines from circular to linear shape. Observe in Fig. 3(b) that the wavefronts leave the cover, as a plane wave. The farfield pattern of the proposed lens is depicted in Fig. 4(b). The results show that the covered antenna has the merit of two highly directive beams, while the single antenna is omnidirectional.

As demonstrated in Fig. 5(a), to verify the scattering characteristics and applicability of the proposed cloak, two antennas are placed in proximity of each other named as antenna 1 and antenna 2 to radiate TM polarized plane wave and cylindrical wave, respectively. It is worth mentioning that the operating frequency of antenna 1 is chosen more than antenna 2, to show the capability of the cloaking effect more clearly. In fact, there is no limitation to select the operating frequency neither for antenna 1 nor antenna 2. However, as discussed in [42], to have an omnidirectional far-field pattern, the radius of the loop antenna should be less than 0.5λ. As the radius becomes more than 0.5λ, the field intensity along the plane of the loop ($\theta = 90°$) reduces and finally it forms a null when $r = 0.61\lambda$. Besides,

when a loop antenna with a radius less than 0.5λ is illuminated with an electromagnetic wave of the corresponding frequency, no significant scattering can be observed. Therefore, the effect of the cloaking layer cannot be distinguished. Three scenarios will be studied as follows: First, antenna 1 radiates in free space while antenna 2 does not exist. Electric field distribution of antenna 1 is depicted in Fig. 5(b). Due to the short distance between the two antennas, scattering from the second antenna will lead to a distortion in the near field pattern (Fig. 5(c)). By employing the designed coating, the second antenna will be cloaked and no scattering will be happened. Fig. 5(d) shows that the proposed cloak converts the loop-family antennas to a PEC surface. It is based on the fact that there will be no scattering when TM polarized waves incident onto a PEC surface, with the electric fields perpendicular to the surface. As a result, the radiated waves from the first antenna will turn around the second antenna without any distortions in the near field pattern.

The far-field results for cloaking performance in the three scenarios are illustrated in Fig. 6. A horn antenna is placed in front of antenna 2, while its beam is directed at $\phi = 0°$. Antenna 2 causes scatterings toward other directions and angles. Therefore, the far-field pattern is increased about $15\,\text{dB}$ around $\phi = 100°$ compared with the free space scenario (Fig. 6). By placing the presented cloak, the far-field pattern will be restored to the free space situation.
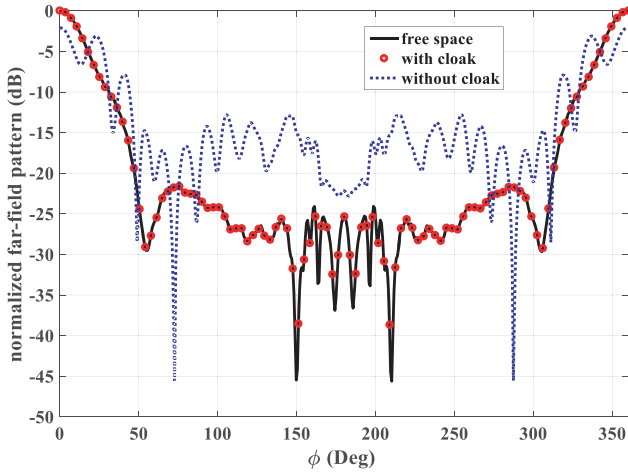

Figure 6. The far-field pattern produced by antenna 1 at 10.5 GHz for three cases: 1) Antenna 1 radiating in free space. 2) Antenna 1 radiating in the presence of the loop-type antenna (antenna 2). 3) Antenna 2 is covered by the proposed cloak.
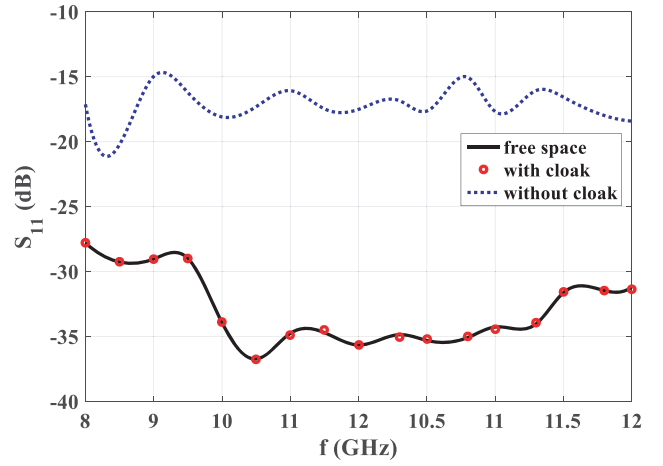
Figure 7. The S-parameter of the horn antenna for three cases illustrated in Fig. 6.

In addition, the loop-type antenna in Fig. 7 causes mutual couplings and distortions in the S-parameters of horn antenna. A comparison is made between the lower and higher frequencies in order to explicitly show the destructive effects of mutual couplings. Coating the loop-type antenna with the proposed layer will eliminate the loading effect and restores its S-parameters to previous values.

As stated before, using quasi-conformal mapping allows minimizing the anisotropy of constitutive materials, leads to the simpler implementation of devices. As demonstrated in Fig. 2, the obtained material is magnetically inhomogeneous and we should first discretize its material parameters to simplify the realization. In Fig. 8, the discrete model of the proposed bi-functional coating layer is presented. The effective permeability of each cell is considered to be constant across the cell and is equal to the average permeability within the cell. Choosing the position at $x = 0.028\,\text{m}$ and $y = 0$ as an example, we will obtain $\mu_r = 0.3$ and $\varepsilon_r = 1$.

In order to realize such a bi-functional coating layer, a composite of SRR-meander line array is utilized as a building block, which is demonstrated in Fig. 8 [8, 9]. To reduce the EM couplings between the building blocks, the SRR and meander line are both printed on two separated dielectric substrates of RO4003C. The SRR is used to control the value of μ_{zz}. Indeed to implement each piece of this coating
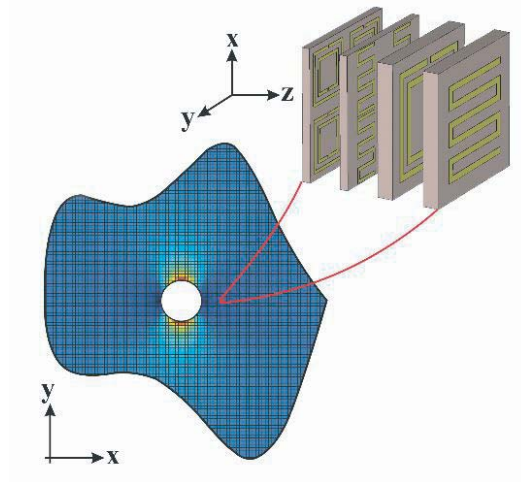
Figure 8. Discretization of the desired permeability to achieve locally homogeneous materials with the proposed meta-atom consists of SRR-meander line array.
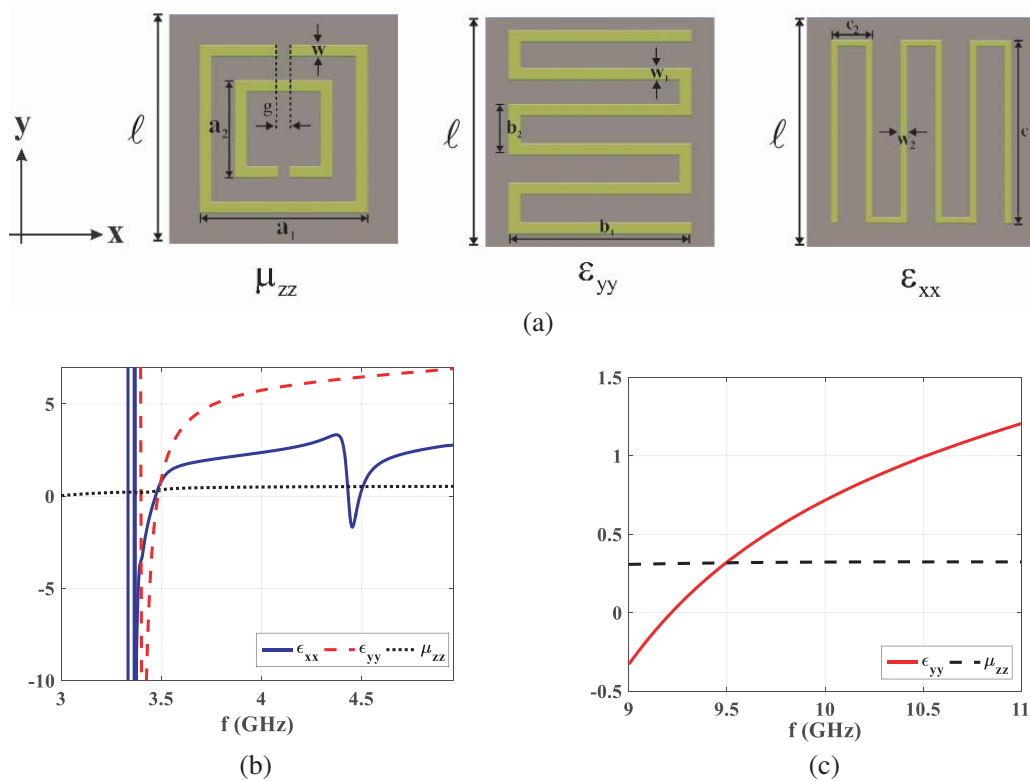

Figure 9. (a) The metamaterial unit-cell geometry with parameters of $\ell = 8.2\,\mathrm{mm}$, $a_1 = 6.6\,\mathrm{mm}$, $a_2 = 5\,\mathrm{mm}$, $w = 0.4\,\mathrm{mm}$, $g = 0.4\,\mathrm{mm}$, $b_1 = 5.9\,\mathrm{mm}$, $b_2 = 1.5\,\mathrm{mm}$, $w_1 = 0.4\,\mathrm{mm}$, $c_1 = 5.6$, $c_2 = 1.6\,\mathrm{mm}$, $w_2 = 0.35\,\mathrm{mm}$ for $f = 3.5\,\mathrm{GHz}$ and $\ell = 4.1\,\mathrm{mm}$, $a_1 = 3.3\,\mathrm{mm}$, $a_2 = 2.3\,\mathrm{mm}$, $w = 0.2\,\mathrm{mm}$, $g = 0.2\,\mathrm{mm}$, $b_1 = 1.94\,\mathrm{mm}$, $b_2 = 0.95\,\mathrm{mm}$, $w_1 = 0.2\,\mathrm{mm}$ for $f = 10.5\,\mathrm{GHz}$. (b), (c) The retrieved material parameters.

layer, the corresponding SRR's geometry should be readjusted to attain the proper permeability value. The SRRs, which are designed to have control over the μ_{zz} value, are oriented in the opposite direction to diminish any bi-anisotropy that might be caused by asymmetry of the structure [43]. Due to the use of these metallo-dielectric structures, the resultant permittivity does not remain one. To overcome

this drawback, the meander line is used to control the value of ε_r. It is worth to mention that as the proposed coating layer should keep its functionalities at two different frequencies (i.e., 3.5 GHz for directivity enhancement and 10.5 GHz for cloaking behavior), the metamaterial building block, consists of two-type SRR-meander lines with different dimensions. Moreover, since the loop antenna radiates an electric field in the azimuthal direction (E_φ), two different meander lines are used at 3.5 GHz, which are oriented back to back with the 90° rotation with respect to each other to control the value of ε_x and ε_y (see Fig. 9). The meta-atom of metamaterial is designed with the CST microwave studio commercial software. For this purpose, a systematic parameter study of the effect of different geometrical parameters on the constitutive material is made. Then the scattering parameters are obtained by assigning the periodic boundary conditions to the lateral walls in both the z- and x-directions. A TM polarized plane wave (with the magnetic field along the z-direction) impinges on the metamaterial blocks. Therefore, the determinant parameters under the TM polarization (i.e., ε_{xx}, ε_{yy} and μ_{zz}) are obtained with the anisotropic retrieval algorithm [44]. This procedure is repeated by changing each geometrical parameter of the meta-atom (shown in Fig. 9(a)) to find their influence on the constitutive parameters. Afterward, the suitable geometrical parameters are obtained, which their results are plotted in Figs. 9(b) and 9(c).

As can be seen in Figs. 9(b) and 9(c), the retrieved results are in good agreement with the required parameters at the frequencies of 3.5 GHz and 10.5 GHz, respectively. As a result, this shows the possibility of realizing the building blocks all over the proposed coating layer through altering the dimensions and parameters described in the caption of Fig. 9.

4. SUMMARY

A novel bi-functional coating layer using quasi-conformal mapping is presented in this paper, which enhances the directivity of the loop-type antenna and cloaks it simultaneously. To obtain material parameters of the coating layer, the Laplace equation is solved numerically. Using quasi-conformal mapping for such layers with Neumann-Dirichlet boundary conditions simplifies the obtained medium to an isotropic material. The full-wave simulations are carried out by COMSOL Multiphysics, which confirm both the cloaking and directivity enhancement functionalities. In addition, far-field patterns and S-parameters are compared to confirm the improvements in antenna characteristics coated with the proposed layer. Finally, to demonstrate the feasibility of our design, a meta-atom of metamaterial is proposed to realize such a bi-functional coating layer. This cloak can be widely used in multiple-antenna environments such as ships and aircraft.

REFERENCES

1. Pendry, J. B., D. Schurig, and D. R. Smith, "Controlling electromagnetic fields," *Science*, Vol. 312, No. 5781, 1780–1782, 2006.
2. Leonhardt, U. and T. G. Philbin, "Transformation optics and the geometry of light," *Progress in Optics*, Vol. 53, 69–152, Elsevier, 2009.
3. Dolin, L. S., "To the possibility of comparison of three-dimensional electromagnetic systems with nonuniform anisotropic filling," *Izv. Vyssh. Uchebn. Zaved. Radiofizika*, Vol. 4, No. 5, 964–967, 1961.
4. Nicolet, A., F. Zolla, and S. Guenneau, "Modelling of twisted optical waveguides with edge elements," *The European Physical Journal Applied Physics*, Vol. 28, No. 2, 153–157, 2004.
5. Rahm, M., D. Schurig, D. A. Roberts, S. A. Cummer, D. R. Smith, and J. B. Pendry, "Design of electromagnetic cloaks and concentrators using form-invariant coordinate transformations of Maxwell's equations," *Photonics and Nanostructures-fundamentals and Applications*, Vol. 6, No. 1, 87–95, 2008.
6. Roberts, D. A., M. Rahm, J. B. Pendry, and D. R. Smith, "Transformation-optical design of sharp waveguide bends and corners," *Applied Physics Letters*, Vol. 93, No. 25, 251111, 2008.
7. Kwon, D. H. and D. H. Werner, "Transformation optical designs for wave collimators, flat lenses and right-angle bends," *New Journal of Physics*, Vol. 10, No. 11, 115023, 2008.

8. Barati, H., M. H. Fakheri, and A. Abdolali, "Experimental demonstration of metamaterial-assisted antenna beam deflection through folded transformation optics," *Journal of Optics*, Vol. 20, No. 8, 085101, 2018.

9. Sedeh, H. B., M. H. Fakheri, and A. Abdolali, "Advanced synthesis of meta-antenna radiation pattern enabled by transformation optics," *Journal of Optics*, Vol. 21, No. 4, 045108, 2019.

10. Chen, H., B. I. Wu, B., Zhang, and J. A. Kong, "Electromagnetic wave interactions with a metamaterial cloak," *Physical Review Letters*, Vol. 99, No. 6, 063903, 2007.

11. Ruan, Z., M. Yan, C. W. Neff, and M. Qiu, "Ideal cylindrical cloak: perfect but sensitive to tiny perturbations," *Physical Review Letters*, Vol. 99, No. 11, 113903, 2007.

12. Yan, M., Z. Ruan, and M. Qiu, "Cylindrical invisibility cloak with simplified material parameters is inherently visible," *Physical Review Letters*, Vol. 99, No. 23, 233901, 2007.

13. Li, J. and J. B. Pendry, "Hiding under the carpet: A new strategy for cloaking," *Physical Review Letters*, Vol. 101, No. 20, 203901, 2008.

14. Ergin, T., N. Stenger, P. Brenner, J. B. Pendry, and M. Wegener, "Three-dimensional invisibility cloak at optical wavelengths," *Science*, Vol. 328, No. 5976, 337–339, 2010.

15. Ma, H. F. and T. J. Cui, "Three-dimensional broadband ground-plane cloak made of metamaterials," *Nature Communications*, Vol. 1, 21, 2010.

16. Fakheri, M. H., H. Barati, and A. Abdolali, "Carpet cloak design for rough surfaces," *Chinese Physics Letters*, Vol. 34, No. 8, 084101, 2017.

17. Xi, S., H. Chen, B. I. Wu, and J. A. Kong, "One-directional perfect cloak created with homogeneous material," *IEEE Microwave and Wireless Components Letters*, Vol. 19, No. 3, 131–133, 2009.

18. Jiang, W. X., H. F. Ma, Q. Cheng, and T. J. Cui, "A class of line-transformed cloaks with easily realizable constitutive parameters," *Journal of Applied Physics*, Vol. 107, No. 3, 034911, 2010.

19. Ma, Y., Y. Liu, L. Lan, T. Wu, W. Jiang, C. K. Ong, and S. He, "First experimental demonstration of an isotropic electromagnetic cloak with strict conformal mapping," *Scientific Reports*, Vol. 3, 2182, 2013.

20. Landy, N. and D. R. Smith, "A full-parameter unidirectional metamaterial cloak for microwaves," *Nature Materials*, Vol. 12, No. 1, 25, 2013.

21. Keivaan, A., M. H. Fakheri, A. Abdolali, and H. Oraizi, "Design of coating materials for cloaking and directivity enhancement of cylindrical antennas using transformation optics," *IEEE Antennas and Wireless Propagation Letters*, Vol. 16, 3122–3125, 2017.

22. Chen, P. Y. and A. Alu, "Mantle cloaking using thin patterned metasurfaces," *Physical Review B*, Vol. 84, No. 20, 205110, 2011.

23. Holloway, C. L., E. F. Kuester, J. A. Gordon, J. O'Hara, J. Booth, and D. R. Smith, "An overview of the theory and applications of metasurfaces: The two-dimensional equivalents of metamaterials," *IEEE Antennas and Propagation Magazine*, Vol. 54, No. 2, 10–35, 2012.

24. Rouhi, K., H. Rajabalipanah, and A. Abdolali, "Multi-bit graphene-based bias-encoded metasurfaces for real-time terahertz wavefront shaping: From controllable orbital angular momentum generation toward arbitrary beam tailoring," *Carbon*, Vol. 149, 125–138, 2019.

25. Yuan, Y., K. Zhang, X. Ding, B. Ratni, S. N. Burokur, and Q. Wu, "Complementary transmissive ultra-thin meta-deflectors for broadband polarization-independent refractions in the microwave region," *Photonics Research*, Vol. 7, No. 1, 80–88, 2019.

26. Zhang, K., Y. Yuan, X. Ding, B. Ratni, S. N. Burokur, and Q. Wu, "High-efficiency metalenses with switchable functionalities in microwave region," *ACS Applied Materials and Interfaces*, Vol. 11, No. 31, 28423–28430, 2019.

27. Monti, A., J. C. Soric, A. Alù, A. Toscano, and F. Bilotti, "Anisotropic mantle cloaks for TM and TE scattering reduction," *IEEE Transactions on Antennas and Propagation*, Vol. 63, No. 4, 1775–1788, 2015.

28. Qin, F. F., Z. Z. Liu, Q. Zhang, H. Zhang, and J. J. Xiao, "Mantle cloaks based on the frequency selective metasurfaces designed by bayesian optimization," *Scientific Reports*, Vol. 8, No. 1, 14033, 2018.

29. Kwon, D. H., "Lossless tensor surface electromagnetic cloaking for large objects in free space," *Physical Review B*, Vol. 98, No. 12, 125137, 2018.

30. Monti, A., J. Soric, M. Barbuto, D. Ramaccia, S. Vellucci, F. Trotta, and F. Bilotti, "Mantle cloaking for co-site radio-frequency antennas," *Applied Physics Letters*, Vol. 108, No. 11, 113502, 2016.

31. Moreno, G., A. B. Yakovlev, H. M. Bernety, D. H. Werner, H. Xin, A. Monti, and A. Alu, "Wideband elliptical metasurface cloaks in printed antenna technology," *IEEE Transactions on Antennas and Propagation*, Vol. 66, No. 7, 3512–3525, 2018.

32. Tang, W., C. Argyropoulos, E. Kallos, W. Song, and Y. Hao, "Discrete coordinate transformation for designing all-dielectric flat antennas," *IEEE Transactions on Antennas and Propagation*, Vol. 58, No. 12, 3795–3804, 2010.

33. Tang, W., Y. Hao, and R. Mittra, "Design of a carpet cloak to conceal an antenna located underneath," *IEEE Transactions on Antennas and Propagation*, Vol. 60, No. 9, 4444–4449, 2012.

34. Ma, H., S. Qu, Z. Xu, and J. Wang, "Numerical method for designing approximate cloaks with arbitrary shapes," *Physical Review E*, Vol. 78, No. 3, 036608, 2008.

35. Hu, J., X. Zhou, and G. Hu, "Design method for electromagnetic cloak with arbitrary shapes based on Laplace's equation," *Optics Express*, Vol. 17, No. 3, 1308–1320, 2009.

36. Jiang, W. X., T. J. Cui, H. F. Ma, X. Y. Zhou, and Q. Cheng, "Cylindrical-to-plane-wave conversion via embedded optical transformation," *Applied Physics Letters*, Vol. 92, No. 26, 261903, 2008.

37. Wu, Q., Z. H. Jiang, O. Quevedo-Teruel, J. P. Turpin, W. Tang, Y. Hao, and D. H. Werner, "Transformation optics inspired multibeam lens antennas for broadband directive radiation," *IEEE Transactions on Antennas and Propagation*, Vol. 61, No. 12, 5910–5922, 2013.

38. Zhang, K., X. Ding, D. Wo, F. Meng, and Q. Wu, "Experimental validation of ultra-thin metalenses for N-beam emissions based on transformation optics," *Applied Physics Letters*, Vol. 108, No. 5, 053508, 2016.

39. Ma, H. F. and T. J. Cui, "Three-dimensional broadband and broad-angle transformation-optics lens," *Nature Communications*, Vol. 1, 124, 2010.

40. García-Meca, C., A. Martínez, and U. Leonhardt, "Engineering antenna radiation patterns via quasi-conformal mappings," *Optics Express*, Vol. 19, No. 24, 23743–23750, 2011.

41. Thompson, J. F., B. K. Soni, and N. P. Weatherill (eds.), *Handbook of Grid Generation*, CRC Press, 1998.

42. Balanis, C. A., *Antenna Theory: Analysis and Design*, John Wiley and Sons, 2016.

43. Jiang, Z. H., M. D. Gregory, and D. H. Werner, "Broadband high directivity multibeam emission through transformation optics-enabled metamaterial lenses," *IEEE Transactions on Antennas and Propagation*, Vol. 60, No. 11, 5063–5074, 2012.

44. Jiang, Z. H., J. A. Bossard, X. Wang, and D. H. Werner, "Synthesizing metamaterials with angularly independent effective medium properties based on an anisotropic parameter retrieval technique coupled with a genetic algorithm," *Journal of Applied Physics*, Vol. 109, No. 1, 013515, 2011.